Mapping interindividual variability of toxicodynamics using high-throughput transcriptomics and primary human hepatocytes from fifty donors

Niemeijer, M.C.; Więcek, W.; Fu, S.; Huppelschoten, S.; Bouwman, R.J.P.; Baze, A.; ... ; Water, B. van de

Citation

Research

Mapping Interindividual Variability of Toxicodynamics Using High-Throughput Transcriptomics and Primary Human Hepatocytes from Fifty Donors

Marije Niemeijer,[1] Witold Więcek,[2] Shuai Fu,[2] Suzanna Huppelschoten,[1] Peter Bouwman,[1] Audrey Baze,[3] Céline Parmentier,[3] Lysiane Richert,[3,4] Richard S. Paules,[5] Frederic Y. Bois,[2] and Bob van de Water[1]

[1]Division of Drug Discovery and Safety, LACDR, Leiden University, Leiden, The Netherlands
[2]Simcyp Division, CERTARA, Sheffield, UK
[3]KaLy-Cell, Plobsheim, France
[4]Zylan, Obernai, France
[5]Division of the National Toxicology Program, NIEHS, NIH, Research Triangle Park, North Carolina, USA

BACKGROUND: Understanding the variability across the human population with respect to toxicodynamic responses after exposure to chemicals, such as environmental toxicants or drugs, is essential to define safety factors for risk assessment to protect the entire population. Activation of cellular stress response pathways are early adverse outcome pathway (AOP) key events of chemical-induced toxicity and would elucidate the estimation of population variability of toxicodynamic responses.

OBJECTIVES: We aimed to map the variability in cellular stress response activation in a large panel of primary human hepatocyte (PHH) donors to aid in the quantification of toxicodynamic interindividual variability to derive safety uncertainty factors.

METHODS: High-throughput transcriptomics of over 8,000 samples in total was performed covering a panel of 50 individual PHH donors upon 8 to 24 h exposure to broad concentration ranges of four different toxicological relevant stimuli: tunicamycin for the unfolded protein response (UPR), diethyl maleate for the oxidative stress response (OSR), cisplatin for the DNA damage response (DDR), and tumor necrosis factor alpha (TNFα) for NF-κB signaling. Using a population mixed-effect framework, the distribution of benchmark concentrations (BMCs) and maximum fold change were modeled to evaluate the influence of PHH donor panel size on the correct estimation of interindividual variability for the various stimuli.

RESULTS: Transcriptome mapping allowed the investigation of the interindividual variability in concentration-dependent stress response activation, where the average of BMCs had a maximum difference of 864-, 13-, 13-, and 259-fold between different PHHs for UPR, OSR, DDR, and NF-κB signaling-related genes, respectively. Population modeling revealed that small PHH panel sizes systematically underestimated the variance and gave low probabilities in estimating the correct human population variance. Estimated toxicodynamic variability factors of stress response activation in PHHs based on this dataset ranged between 1.6 and 6.3.

DISCUSSION: Overall, by combining high-throughput transcriptomics and population modeling, improved understanding of interindividual variability in chemical-induced activation of toxicity relevant stress pathways across the human population using a large panel of plated cryopreserved PHHs was established, thereby contributing toward increasing the confidence of *in vitro*-based prediction of adverse responses, in particular hepatotoxicity. https://doi.org/10.1289/EHP11891

Introduction

One of the main responsibilities of the liver is the metabolism of endogenous and xenobiotic substances making the liver susceptible to chemical-induced injury through exposure to environmental toxicants or drugs. Indeed, the development of liver injury is one of the most frequent adverse outcomes in *in vivo* chemical safety testing.[1,2] Environmental toxicants, such as pesticides, volatile organochlorine chemicals, perfluorinated alkyl substances, aflatoxins, or microcystins, are known to contribute to the development of liver disease, including development of fatty liver disease and hepatocellular carcinoma.[3–5] Also, particular drugs are known to induce liver injury, which is one of the main reasons for drug withdrawal from the market.[6] Therefore, it is key to improve prediction of chemical-induced hepatotoxicity

causing the development of liver disease and accurately account for interindividual variability within the human population.

For the evaluation of liver injury by environmental toxicants or drugs, primary human hepatocytes (PHHs) are currently considered to be the gold standard of tissue culture models for human liver toxicity.[7] Despite their disadvantages, such as dedifferentiation and source limitations, they closely resemble human hepatocytes *in vivo*, allowing for the study of chemical-induced liver injury.[8] Therefore, PHHs from different donors form an excellent basis to get a deeper understanding of interindividual variability in toxicodynamic responses.

For chemical safety assessment, a default uncertainty factor (UF) of 10 is used for interindividual variability, with the goal to equally account for toxicokinetic (TK) and toxicodynamic (TD) variability each with a standard UF of 3.16.[9] The original value of 10 was based on expert judgement and anecdotal evidence.[10,11] Research then focused on justifying those values, because they had already been widely adopted and hard to change. Statistical justifications were found using distributions of the slopes of probit analyses (which, in theory, measure interindividual variability), but the data came from acute toxicity experiments in inbred laboratory animals.[11] The focus shifted on separating TK from TD variability and finding the coverage (fraction of the population protected) of the factor 10, particularly in human sensitive populations, such as children.[12] A decisive advance came from meta-analytic reviews of metabolic variability in humans, but they focused on TK, noting that TD data were scarce and inadequate (Dorne[13] and related papers). While the variability of TK properties has received much investigation and are integrated in computational TK prediction models,[14–17] the quantitative aspects of interindividual TD variability are still poorly understood. Recent studies have started to tackle TD variability (although in fact,

---

Note to readers with disabilities: *EHP* strives to ensure that all journal content is accessible to all readers. However, some figures and Supplemental Material published in *EHP* articles may not conform to 508 standards due to the complexity of the information being presented. If you need assistance accessing journal content, please contact ehpsubmissions@niehs.nih.gov. Our staff will work with you to assess and meet your accessibility needs within 3 working days.

in vitro TK variability may contaminate such results), using Bayesian statistical methods.[18–20] However, they examined only a very limited set of phenotypic toxicity end points. Whether the UF of 10 is enough to capture the full human population variability for various toxicity pathways is still unclear, and that hampers reliable risk assessments. There is a need for data-driven interindividual UFs, which are both chemical and end point specific.

During chemical-induced stress, cellular defensive mechanisms are activated to restore homeostasis. Well-known stress responses are the oxidative stress response in reaction to accumulation of reactive oxygen species (ROS) regulated by nuclear factor, erythroid 2 like 2 (*NFE2L2*/NRF2)[21,22]; the unfolded protein response (UPR) activated upon accumulation of misfolded proteins in the endoplasmic reticulum (ER) regulated by three sensors, endoplasmic reticulum to nucleus signaling 1 (*ERN1*/IRE1α), activating transcription factor 6 (ATF6), and eukaryotic translation initiation factor 2 alpha kinase 3 (*EIF2AK3*/PERK)[23–25]; the DNA damage response mediated by tumor protein P53 (*TP53*/P53) signaling upon DNA damage[26–28]; and NF-κB signaling upon inflammatory conditions.[29,30] Monitoring the activation of these adaptive stress responses upon chemical exposure can give insight into liver injury liabilities of chemicals as well as the underlying modes-of-action.[31,32] Because of the protective functions of adaptive stress responses, interindividual variations in their activities affect adverse outcomes such as liver injury.[33] Quantitative insight in these variations among the human population would allow the derivation of data-driven toxicodynamic UFs specifically for each type of stress response, thereby enabling better predictions of liver injury liabilities.

Omics approaches, such as transcriptomics, are powerful tools to fully map differences in adaptive stress response signaling networks across different patients. Several studies have already used transcriptomics approaches to compare differences between chemical-induced stress responses in different liver cell culture models.[34,35] Due to advances in this area, novel approaches such as targeted templated oligo-sequencing (TempO-Seq) technology can now be used, which allow for transcriptome mapping of gene sets of interest in a high-throughput fashion.[36,37] This allows large-scale population studies and accurate analyses of interindividual variability in transcriptomic perturbations for the improvement of liver injury liability assessment. When combining experimental transcriptomic data with population modeling, an estimate of the variance across the entire population can be derived, an approach taken by Blanchette et al.[20] for the evaluation of the variance in chemical-induced cardiotoxicity.[20,38]

Here, to map the interindividual variability in stress response activation upon chemical exposure, we profiled the transcriptome for over 8,000 samples covering a large panel of 50 cryopreserved PHHs derived from different individuals and exposed to a broad concentration range of specific stress response–inducing compounds, namely diethyl maleate, tunicamycin, cisplatin, and tumor necrosis factor alpha (TNFα) to induce the oxidative stress, UPR, DNA damage, and NF-κB signaling, respectively. Chemical-induced perturbation of the transcriptome was evaluated upon 8 and 24 h of exposure using TempO-Seq technology.[36] In combination with population modeling, these data allowed us to evaluate the influence of PHH panel sizes on the correct estimation of interindividual variance in chemical stress responses and exemplify the need of data-driven toxicodynamic UFs, which will contribute to improved prediction of chemical-induced liver injury liabilities.

Methods

Cell Culture

Plateable cryopreserved PHHs[39] were derived from the safety margin of liver tissue resected in case of hepatic tumors from 54 different individuals (KaLy-Cell) with permission of the national ethics committees and regulatory authorities (Excel Table S1). For plating, PHHs were thawed in a warm water bath at 37°C and diluted in pre-warmed universal cryopreservation recovery medium (UCRM) (IVAL) followed by centrifugation at $170 \times g$ for 20 min at room temperature (RT). Thereafter, cell pellet was diluted in seeding universal primary cell plating medium (UPCM) (IVAL), and viability was assessed using the Trypan blue exclusion method.[40] Cells were plated at a density of 70,000 cells in 100 μL per well in 96-well BioCoat Collagen I Cellware plates from Corning. After 6 h, medium was refreshed with seeding UPCM medium. PHHs showing <70% confluency 24 h after plating were discarded from further analysis leading to a panel of PHHs derived from in total 50 individuals. Characteristics of these PHHs are depicted in Figure S1 and Excel Table S1, including information regarding confluency and day of plating. Demographic information of donors was given by the hospital and received simultaneously with the resection. To evaluate variability in dedifferentiation upon culturing of PHHs, PHHs in suspension directly upon thawing or from matching snap-frozen liver tissue were also analyzed derived from eight individuals (Excel Table S1, column WT analyzed).

Cell Treatment

Prior to compound exposure, PHHs were first washed after 24 h of attachment using $1 \times$ phosphate-buffered saline (PBS) to remove unattached cells. Exposures were done using William's E medium supplemented with 100 U/mL penicillin and 100 μg/mL streptomycin. PHHs were exposed to four reference compounds in a broad concentration range known to induce specific stress response pathways (Table S1), namely tunicamycin (0.0001–10 μM) and diethyl maleate (1–3,300 μM) from Sigma, TNFα (0.1–33 ng/mL) from R&D systems, and cisplatin "Ebewe" 1 mg/mL concentrate for solution for infusion (0.1–100 μM).[32] To evaluate variability in stress response activation by hepatotoxicants, PHHs were exposed to a broad concentration range ($1–100 \times$ Cmax) of acetaminophen, propylthiouracyl, nitrofurantoin, ticlopidine, nefazodone, and diclofenac (Table S1) from Sigma. All compound stocks, except for TNFα and cisplatin, were prepared using dimethylsulfoxide (DMSO) from BioSolve and stored at −20°C. End concentration of DMSO in all conditions were kept identical at 0.2%. TNFα was reconstituted in $1 \times$ PBS containing 0.1% bovine serum albumin at a concentration of 10 μg/mL.

Cell Viability

To evaluate cytotoxicity, lactate dehydrogenase (LDH) leakage was evaluated after 24 h of exposure for all compounds and concentrations tested in the culture medium of PHHs using a cytotoxicity detection kit from Roche (catalog number 11644793001) according to instructions by provider. As a positive control, PHHs incubated for 5 min with 1% triton were taken along. Collected medium was stored at 4°C for a maximum of 3 d before analysis. Upon analysis, medium samples were diluted $10 \times$ with $1 \times$ PBS and measured in triplicate. Absorbance was measured at 490 nm with a VICTOR plate reader (PerkinElmer). Cell viability was determined for three biological replicates for each condition for each PHH.

Targeted Sequencing

The transcriptome was analyzed after exposure to the four reference compounds (tunicamycin, diethyl maleate, TNFα, or cisplatin in a broad concentration range) for 8 and 24 h for the whole panel of 50 PHHs and with the hepatotoxicants for the identified three most and least sensitive PHHs in stress response activation (acetaminophen, propylthiouracyl, nitrofurantoin, ticlopidine, nefazodone, and

diclofenac from 1 to $100 \times$ Cmax) for 24 h. The transcriptome was analyzed using the targeted TempO-Seq technology (BioSpyder Technologies, Inc.). First, cells were washed with $1 \times$ PBS and lysed with 50 μL $1 \times$ TempO-Seq lysis buffer (provided by BioSpyder) per well. Lysates were incubated for 15 min at RT and stored at $-80°C$. Samples were shipped for TempO-Seq analysis[36] using the S1500+ gene set of National Institute of Environmental Health Sciences (NIEHS)[41] supplemented with additional stress response relevant genes (Excel Table S2) at BioSpyder and sequenced using a HiSeq 2,500 ultrahigh-throughput sequencing system (Illumina). For each condition and PHH, three biological replicates were analyzed derived from different wells on separate plates on the same experimental day. To evaluate variability in dedifferentiation, samples from PHHs in suspension directly upon thawing, snap-frozen liver tissue, or PHHs grown two-dimensional (2D) for 24 h derived from the identified most or least sensitive PHHs from in total eight individuals were analyzed using the targeted whole-transcriptome panel in combination with TempO-Seq technology (BioSpyder) (Excel Table S2). Datasets are available in the BioStudies Database (http://www.ebi.ac.uk/biostudies) under accession numbers S-TOXR1035, S-TOXR1036 and S-TOXR1705.

Transcriptomics Dose-Response Analysis and Statistics

For the analysis of TempO-Seq transcriptome data, as a first step, reads were aligned by BioSpyder technologies using the TempO-Seq R package. Derived raw counts were normalized using R version 4.0.0 (R Development Core Team) and the DESeq2 R package[42] with the functions DESeqDataSetFromMatrix (design = ~1), estimateSizeFactors, and counts (normalized = TRUE) using default settings and subsequently log2 transformed. For each PHH and condition, three biological replicates were analyzed and represented as the mean. A library size cut-off was used of 100,000 counts to eliminate samples having a low amount of total counts (Figure S2). Pearson's correlation of the gene expression profiles between replicates and samples was calculated using the cor function from the stats R package (R Development Core Team). To evaluate variability in sensitivity for stress response activation, benchmark concentration (BMC) modeling was done using the BMDExpress 2 software version 2.2 developed by Sciome LCC and NIEHS/NTP/EPA.[43,44] Dose response modeling was done for each gene and sample using various models (exponential 2 to 5, linear, polynomial 2, Hill, and power model). The best model was selected using the lowest Akaike information criterion (AIC) and a goodness-of-fit p-value >0.05. The Hill model was excluded when the κ parameter was lower than one-third of lowest tested concentration. The BMC was defined as the concentration at which one standard deviation (SD) of increase in gene expression was observed. For each reference compound, the top 50 activated genes across the PHH panel were defined based on both the BMC and the maximal fold change across concentration range (maxFC) (Excel Table S2). First, genes were ranked for both BMC and maxFC followed by calculation of the sum of both ranks. Based on this sum of both ranks, the top 50 genes were selected. The median BMC and maxFC were calculated based on these top 50 genes for each PHH. To classify PHHs for their sensitivity, a sensitivity score was calculated based on the sum of the ranking of the median BMCs and maxFC at both time points for the top 50 genes for each reference compound. Principal component analysis (PCA) was done using prcomp from the stats R package (R Development Core Team). Panther classification system version 17.0 (www.pantherdb.org/) was used for the evaluation of enrichment of GO terms for biological processes using the top 30 genes affecting PC1 of PCA.[45,46] Hierarchical clustering based on Euclidean distance and Wards method was done using the R package pheatmap.[47] Significant differences between PHHs with or without certain disease backgrounds, from patients with any type of cancer or liver pathologies including

liver cancer, were calculated using unpaired Student's t test represented as [*]$p < 0.1$, [**]$p < 0.05$, and [***]$p < 0.01$. Data analysis and visualization was done using R version 4.0.0 (R Development Core Team) and Rstudio with the following R packages: DESeq2 v1.28.1,[42] pheatmap v1.0.12,[47] ggplot2 v3.3.3,[48] data.table v1.14.0,[49] dplyr v1.0.5,[50] reshape2 v1.4.4,[51] and stats R v3.4.1. To evaluate difference in pathway activation between different PHHs, gene set enrichment analysis (GSEA) in combination with Gene Ontology (GO) gene sets version 7.1[52] retrieved from the MSigDB was performed using the maxFC as input in the GSEA software version 4.0.3 (derived from joint project of UC San Diego and Broad Institute).[53,54] Visualization of GSEA results was done using Cytoscape version 3.8.1 software[55] in combination with EnrichmentMap[56] and WordCloud.[57]

Population Statistical Modeling

The BMC-maxFC values distributions were modeled in a Bayesian hierarchical framework. We were interested *a priori* by intersubject variability; therefore, our primary observational unit was the individual donor. Genes were considered as exchangeable; independent and identically distributed.

Examination of the BMC and maxFC values clearly showed that they were clustered in two (positive vs. negative maxFC values, always present because genes with null or small maxFC values would not have been retained) or four groups (combinations of positive vs. negative maxFC values with low or high BMC values) (see Figure S15A). Therefore, at the level of the ith subject, we assumed that the counts n_{ik} of genes falling in the kth of the K (equal to either two or four) predefined clusters followed by a multinomial distribution:

$$n_i = (n_{i1}, \ldots, n_{iK}) \sim \text{Multinomial}(p_{i1}, \ldots, p_{iK}). \quad (1)$$

At the population level, the subjects' multinomial probabilities were softmax-transformed, and the corresponding parameters β were assumed to be multivariate-normal-distributed around a population mean μ with covariance matrix Ω.

$$p_{ik} = \frac{\exp(\beta_{ik})}{\sum_{j=1}^{K} \exp(\beta_{ij})}, \quad (2)$$

$$\beta_{i1} = 0, \quad (3)$$

$$(\beta_{i2}, \ldots, \beta_{iK}) \sim N_{K-1}(\mu, \Omega). \quad (4)$$

The prior on each element of μ was a vague normal distribution:
$$\mu_k \sim N(0,5). \quad (5)$$

The prior on Ω was a Cauchy-LKJ (Lewandowski-Kurowicka-Joe) distribution with a Cauchy-distributed diagonal vector of standard deviations θ:

$$\theta_k \sim \text{Cauchy}(0,2.5) \quad (6)$$

and an LJK-distributed prior on the correlation matrix L:

$$L \sim \text{LKJ}(3). \quad (7)$$

The *Stan* statistical software was used to obtain a posterior sample of μ, θ, and L values by Hamiltonian Monte Carlo simulations.

Still at the ith subject level, we modeled independently for each cluster the joint distribution of genes' BMCs (noted x in the following) and maxFCs (noted y) values as a bivariate lognormal distribution. We took the absolute value of negative maxFC values before log-transformation:

$$\{\log(x_i), \log[abs(y_i)]\} \sim N_2[(\upsilon_{xi}, \upsilon_{yi}), \Delta_i], \tag{8}$$

with Δ defined as

$$\Delta_i = \begin{pmatrix} \sigma_{xi} & \rho_i \\ \rho_i & \sigma_{yi} \end{pmatrix}. \tag{9}$$

At the population level, we modeled the distributions of subjects' means υ_{xi} and υ_{yi}, of the standard deviations σ_{xi} and σ_{yi}, and of the correlation coefficient ρ_i as normal around their population counterparts:

$$\upsilon_{xi} \sim N(\upsilon_x, \sigma_a), \tag{10}$$

$$\upsilon_{yi} \sim N(\upsilon_y, \sigma_b), \tag{11}$$

$$\sigma_{xi} \sim N(\sigma_x, \sigma_c), \tag{12}$$

$$\sigma_{yi} \sim N(\sigma_y, \sigma_d), \tag{13}$$

$$\rho_i \sim N(\rho, \sigma_e). \tag{14}$$

The standard deviations σ_a, σ_b, σ_c, σ_d, and σ_e were all assigned a half normal prior with SD 0.2. The other priors were:

$$\upsilon_x \sim \text{Uniform}(-5, 7), \tag{15}$$

$$\upsilon_y \sim \text{Uniform}(-11.5, 5), \tag{16}$$

$$\sigma_x \sim \text{Halfnormal}(1), \tag{17}$$

$$\sigma_y \sim \text{Halfnormal}(1), \tag{18}$$

$$\rho \sim \text{Uniform}(-1, 1). \tag{19}$$

All of the above priors are weakly informative, as suggested for example by Gelman.[58] All model parameters (265 parameters in total for each chemical exposure) were jointly estimated from the data with Metropolis-Hastings Markov chain Monte Carlo simulation, using the *GNU MCSim* software version 6.1.0.

Predictive Simulations

The above model, after calibration with the data from a panel of 50 PHH donors, can be used as a generative model to simulate virtual *in vitro* assays of various sizes. For a given panel size, BMC and maxFC values expected for any donor can be simulated by Monte Carlo sampling using the posterior estimates obtained as described above (with inverse transformations to obtain BMC and maxFC values in natural space). For model checking, one assay of size 500 was simulated. To assess the effect of panel size on the accuracy and precision of interdonor variability estimates, we first simulated 1,000 assays on virtual panels of 2,000 PHH donors. For each assay, we calculated the coefficients of variation (CVs) of BMC and maxFC values simulated. With 1,000 assays, we obtain a distribution of large-sample (2,000 donors) CV values, assuming that the BMC-maxFC values were correctly modeled. Similar assay simulations were performed for smaller panel sizes (3, 4, 5, 6, 7, 8, 10, 12, 14, 16, 20, 24, 28, 32, 36, 40, and 50 donors), and distributions of BMC and maxFC CVs were obtained for each panel size.

Results

Variability in Basal Gene Expression across PHH Panel

Since PHH show dedifferentiation in cell culture, as an initial step, the variability in dedifferentiation of PHHs derived from different individuals during culture was evaluated (Figure 1A,B). For this purpose, we used whole-transcriptome targeted TempO-Seq analysis of liver tissue and derived cryopreserved PHHs in suspension directly upon thawing or cultured in 2D for 24 h for eight different individuals. Principal component analysis (PCA) showed the greatest variability between individuals for PHHs in suspension (Figure 1A,B). Noticeably, the transcriptome of PHHs cultured in 2D was more like liver tissue compared to PHHs in suspension for principal component 1, representing 60.9% of the total variance (Figure 1A). This was supported by Pearson's correlation analysis (Figure S3; data in Excel Table S22 and S23). GO enrichment analysis using Panther software showed that genes mostly affecting PC1 were involved in metabolic processes (*TMEM70*, *GLYAT*) and response to wounding and inflammatory signaling (*FGA*, *TFPI*, *HLA-E*) (Excel Table S3). This may imply that PHHs in suspension that were freshly thawed needed recovery time upon thawing and, therefore, were temporarily more divergent from liver tissue regarding the transcriptome. However, when only considering liver-related genes, both PHHs cultured in 2D or in suspension were similarly distinct from liver tissue for both principal components, although the latter was more variable (Figure 1B). Genes involved in metabolism, such as *CYP3A4*, *CYP2C8*, and *UGT2B7* were mostly differently expressed between liver tissue and PHHs, either cultured in 2D or in suspension.

Next, we evaluated differences in gene expression for a panel of PHHs derived from 50 individuals cultured for 24 h in 2D for all genes (Figure 1C), liver-related genes (Figure 1D), or stress response-related genes (Figure S4). Gene lists can be found in Excel Table S2. PHHs from some individuals showed altered expression for genes dominating the variance across the first principal component based on all genes, such as *DDIT4*, a regulator of mTOR activity induced upon various stress conditions (Figure 1C). In addition, variability in various phase-I enzymes such as *CYP3A4* was observed across the panel of PHHs mostly affecting the second principal component for liver-related genes (Figure 1D; Figure S5; data in Excel Table S17 and S18). Also, large variability was seen in the expression of *CCL2*, a chemokine involved in the recruitment of monocytes and basophils, affecting the principal components for all genes (Figure 1C), but also more specifically UPR and NF-κB signaling related genes (Figure S4).

Difference in Sensitivity toward Chemical-Induced Cell Death

To evaluate the interindividual variability in chemical-induced cellular stress responses across the panel of 50 PHH cultures, PHHs were exposed for 8 or 24 h to broad concentration ranges of specific stress inducers: diethyl maleate (DEM) for the oxidative stress response, tunicamycin (TUN) for the UPR, cisplatin (CPT) for the DNA damage response, and TNFα for inflammatory NF-κB signaling (Figure 1E). Great difference in viability, measured by LDH leakage, was only observed between PHHs from different individuals following 24 h exposure at the highest concentration of DEM, where significant induction of cell death was observed for a subset of PHHs while other PHHs did not show viability loss at all (Figure 1F). The other compounds did not lead to significant loss of viability upon 24 h of exposure, although some PHHs were more sensitive, such as R1232T and S1295T, resulting in a minor LDH leakage at the highest concentrations.

Interindividual Variability in Chemical-Induced Stress Response Activation

Next, the effects of 8 or 24 h of chemical exposure (DEM, TUN, CPT, TNFα) on the PHH transcriptomes were analyzed. To evaluate the difference in variability within replicates and between
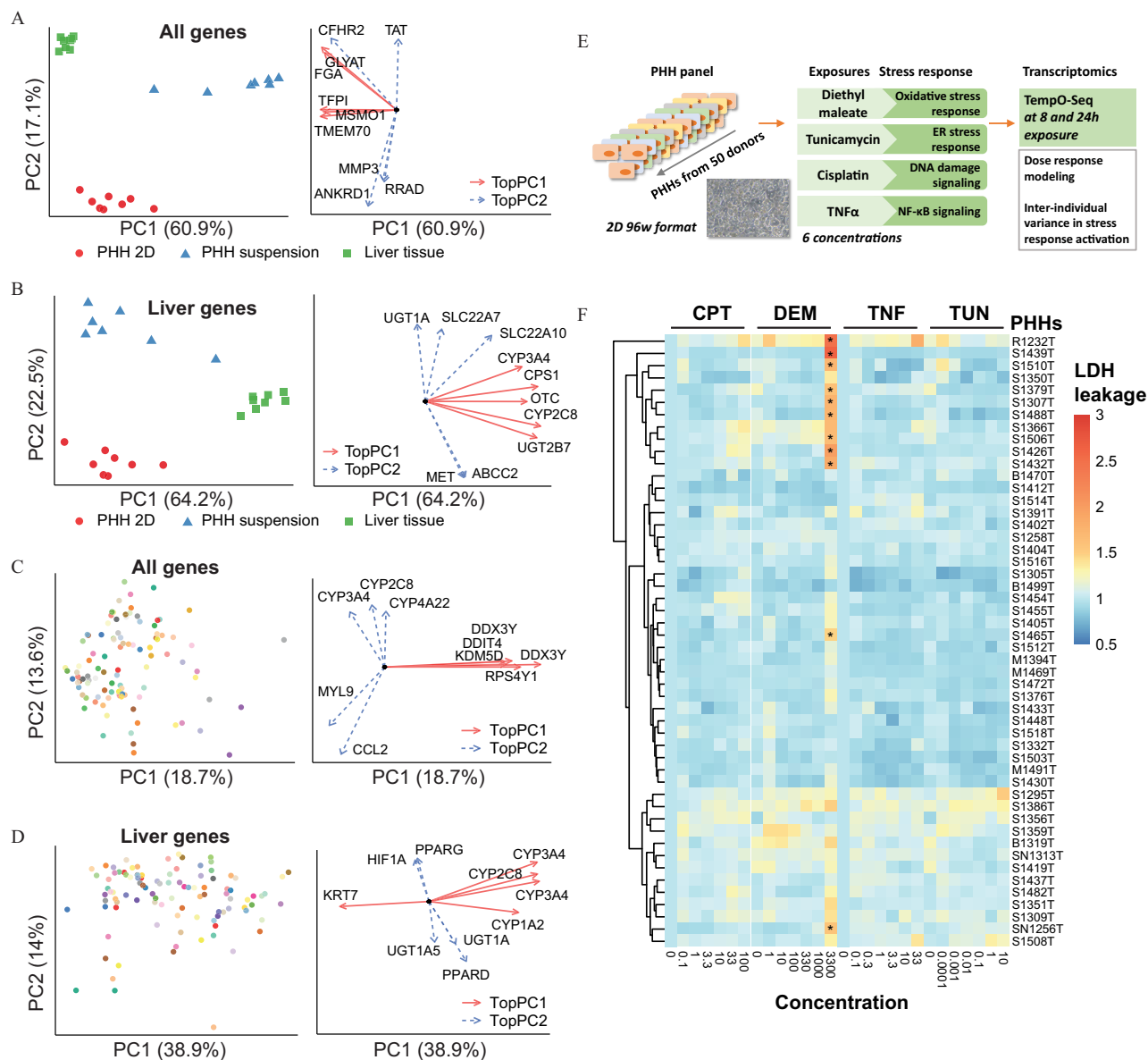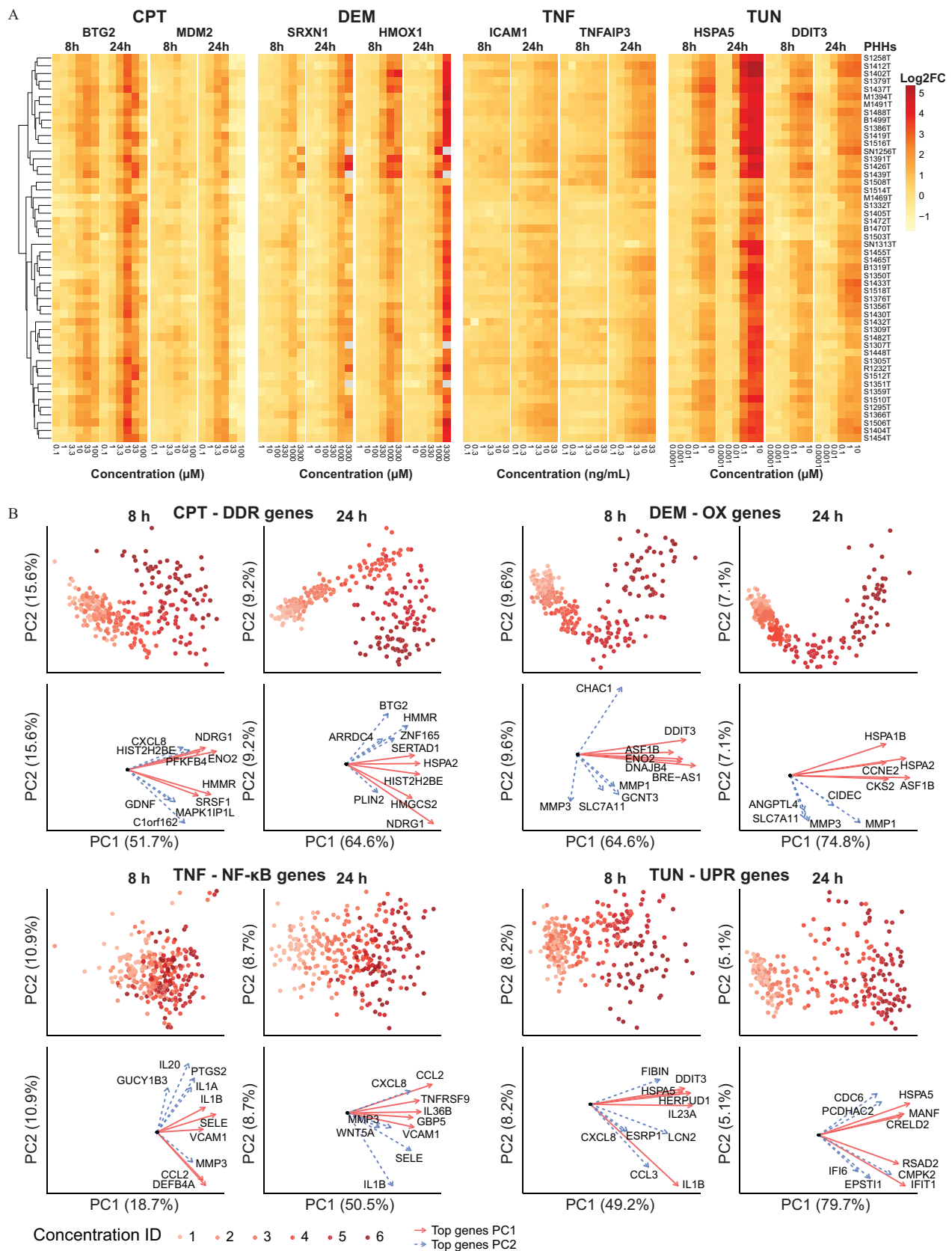
Figure 1. Characterization of the interindividual variability in response to stress-inducing exposures utilizing a large panel of primary human hepatocytes (PHHs) derived from 50 individuals. (A–D) Left panel: Principle component analysis (PCA) based on gene expression as log2 normalized counts. Right panel: Top 5 genes mostly determining PC1 or 2 depicted as vectors representing contribution and PC orientation. (A,B) PCA of liver ($n = 8$), PHHs in suspension ($n = 7$) or grown as 2D ($n = 8$) based on all genes (A) or liver-related genes (B) in a whole-transcriptome panel. (C,D) PCA of panel of 50 PHHs depicted in different colors based on all genes (C) or liver-related genes (D) of S1500+ gene set of NIEHS[41] supplemented with additional stress response relevant genes (Excel Table S2). (E) Schematic representation of experimental setup. (F) LDH leakage (normalized with medium negative controls) upon exposure to diethyl maleate (DEM), tunicamycin (TUN), cisplatin (CPT), and TNFα in wide concentration range for 24 h across panel of PHHs. Concentrations shown in μM for DEM, TUN, and CPT, and ng/mL for TNFα. Data is reported in Excel Table S8. Significant differences were calculated using two-way ANOVA with Bonferroni's multiple comparison correction represented as $^*p < 0.001$. $n = 3$. Note: 2D, two-dimensional; ANOVA, analysis of variance; LDH, lactate dehydrogenase; NIEHS, National Institute of Environmental Health Sciences; TNFα, tumor necrosis factor alpha.

different PHHs in general, Pearson's correlations were calculated between the gene expression profiles of each replicate vs. the mean of replicates and between PHHs from each donor vs. the mean of all donors. This showed lower correlations between different PHHs than between replicates for all donors (Figure S2B,C; data in Excel Table S15 and S16). Exposure to the oxidative stress-inducing compound DEM resulted in clear upregulation of NRF2 target genes *HMOX1* and *SRXN1* at concentrations ranging from 330 μM to 3,300 μM for all PHH donors for both time points compared to solvent control (Figure 2A; individual replicates are shown in Figure S6; data in Excel Table S19). Cisplatin-induced DNA damage signaling in the panel of PHHs was most profound at a

concentration of 10 μM upon 24 h of exposure compared to solvent control, where in general the highest upregulation of P53 target genes *BTG2* and *MDM2* was observed. PHHs showed variable responses, where some PHH donors showed *BTG2* or *MDM2* upregulation already at a cisplatin concentration of 1 μM compared to solvent control, while others required higher amounts of this compound. Regarding the UPR induced by TUN, induction of both the adaptive gene *HSPA5* and pro-apoptotic related gene *DDIT3* was observed at a concentration of 0.01 μM or higher compared to solvent control at the 24 h time point. Some PHHs showed already strong upregulation of both genes at 0.01 μM of TUN, while other PHHs only showed
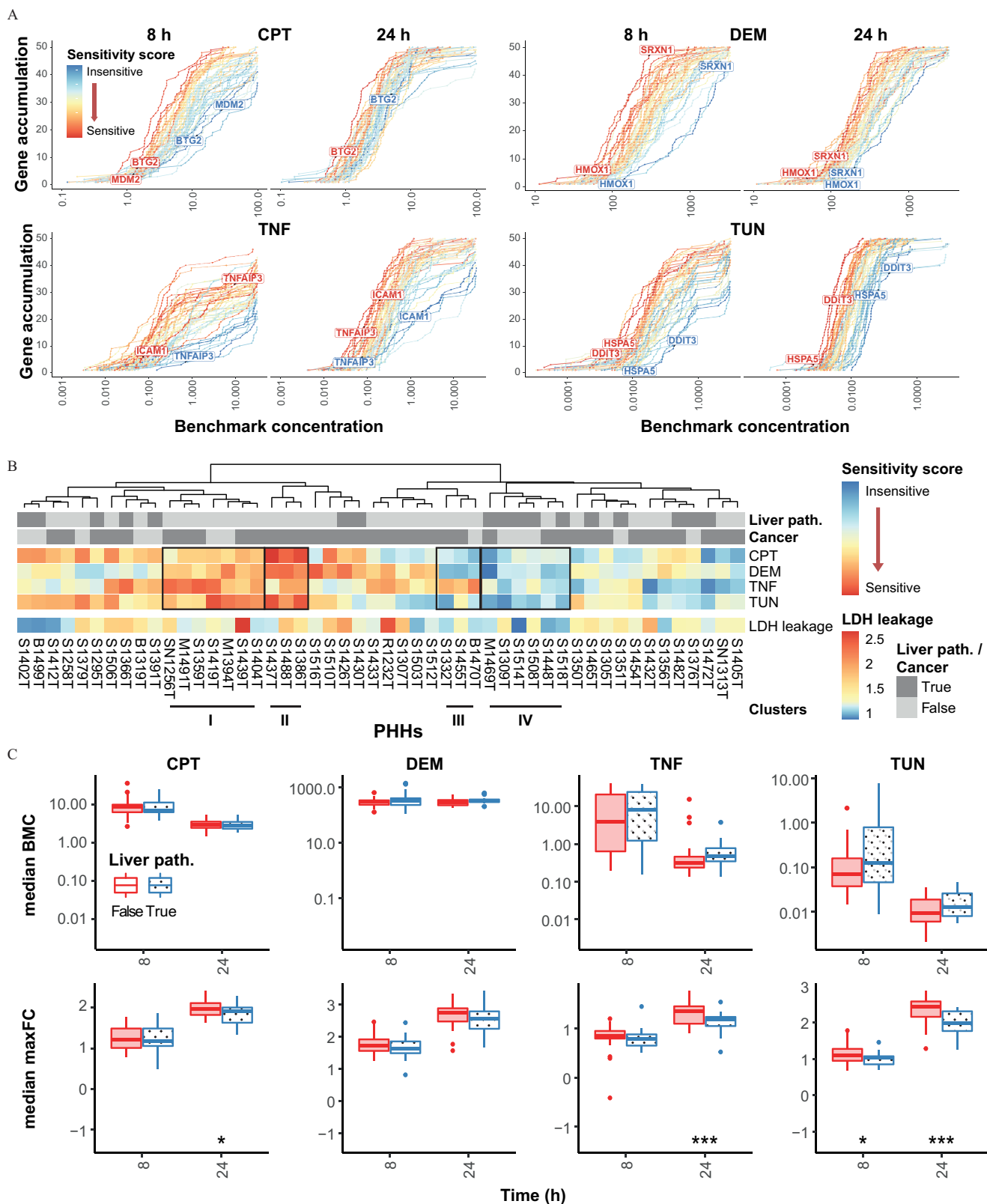
Figure 2. Interindividual variability in concentration-dependent stress response activation. (A) Hierarchical clustering of log2 fold change in gene expression of key genes for each evaluated stress response pathway of panel of primary human hepatocytes (PHHs) exposed to reference compounds compared to solvent control. Data is reported in Excel Table S9. (B) Principle component analysis (PCA) based on log2 fold changes of stress responsive genes of panel of PHHs exposed to diethyl maleate (DEM), tunicamycin (TUN), cisplatin (CPT), and TNF (TNFα) compared to solvent control. Top 5 genes mostly determining PC1 or 2 depicted as vectors representing contribution and PC orientation. $n = 3$. Note: DDR, DNA damage response; OX, oxidative stress response; TNFα, tumor necrosis factor alpha; UPR, unfolded protein response.

Figure 3. Benchmark concentration distributions across panel of primary human hepatocytes (PHHs) and influence of liver disease status. (A) Distribution of benchmark concentrations (BMC) of top 50 stress responsive genes for each compound; diethyl maleate (DEM), tunicamycin (TUN), cisplatin (CPT), and TNF (TNFα) compared to solvent control. Lines represent the different PHHs within panel where the color indicates the sensitivity score (sum of the ranking of the median BMCs and maxFC of top 50 stress responsive genes at both time points). BMC concentrations shown in μM for DEM, TUN, and CPT and ng/mL for TNF. (B) Hierarchical clustering of the sensitivity score for the panel of PHHs for each treatment. The LDH leakage is shown of 3,300 μM DEM at 24 h and the disease status. (C) Boxplots of median BMC or maximal fold change across concentration range (maxFC) of top 50 stress responsive genes of exposure for each treatment for PHHs with or without liver disease status (including liver cancer). BMCs are in μM for DEM, CPT, TUN and in ng/mL for TNF. Data represented as the median, first and third quartile ± 1.5 * interquartile range. Data shown is reported in Excel Table S4–6. Significant differences between PHHs from donors with and without liver pathology were calculated using unpaired Student's t test represented as $^*p < 0.1$, $^{**}p < 0.05$, $^{***}p < 0.01$. $n = 3$. Note: LDH, lactate dehydrogenase; TNFα, tumor necrosis factor alpha.

upregulation at 1 μM or higher, suggesting particularly large differences in the UPR response of different individuals. Upon TNFα exposure to study variability in inflammation signaling, NF-κB target genes *ICAM1* and *TNFAIP3* were induced in a concentration-dependent manner compared to solvent control. For most of the PHHs, induction was observed at 1 ng/mL and higher when exposed for 24 h. Some PHHs showed induction at the lowest concentration of 0.1 ng/mL [e.g., PHH donor S1488T with a benchmark concentration (BMC) of 0.02 and 0.3 ng/mL for TNFAIP3 at 8 and 24 h; Excel Table S4], while other PHHs were less responsive to TNFα exposure (e.g., PHH donor S1472T with a BMC of 48 and 1.7 ng/mL for TNFAIP3 at 8 and 24 h; Excel Table S4).

Subsequently, we selected the top 50 most strongly responsive genes at the lowest effective concentration (Excel Table S2) of each stress response reference compound. The interindividual variability in the concentration-dependent induction of these top 50 genes for each stress response was evaluated by PCA ([Figure 2B](#)). In general, for all compounds, a clear concentration-dependent shift was observed for all PHHs. Most variability was observed between different PHHs for TUN-induced UPR genes and TNFα-induced NF-κB-related genes, mainly driven by variable expression of cyto- or chemokines such as *IL1B*. Since PHHs were plated on different days in batches of six to nine PHH donors, PCA was done to evaluate difference in response between different plating days among the PHHs (Figure S7). The concentration-dependent shift observed was not batch specific, where PHHs from different batches showed a similar trend.

Interindividual Differences in Points-of-Departure of Stress Response Activation

To evaluate the interindividual variability in sensitivity to chemical-induced stress response activation, we defined BMCs at which the top 50 most strongly responsive genes for each specific compound showed an increase of 1 standard deviation in gene expression (Excel Table S4). Upon dose response modeling, we observed large differences in the gene-specific BMCs between different PHHs ([Figure 3A](#)). In general, most variability was observed at 8 h of exposure, while at 24 h, the response was more stable across the PHH panel. Large shifts in the BMC distribution could be observed especially at the 8 h time point, with medians varying 864-, 259-, 13-, and 13-fold for TUN, TNFα, DEM, and CPT, respectively ([Table 1](#); Excel Table S5 and S6; Figure S8). This means that BMC estimations could shift significantly depending on which PHHs were used in chemical toxicity testing at early time points. Variability could also be observed in the distribution of the maxFC of the top 50 most strongly responsive genes among the different PHHs, where compound sensitivity correlated positively with levels of upregulation (Figure S9). To

distinguish between intra- and interindividual variability, BMC and maxFCs were also defined for each individual biological replicate. Here, variability between biological replicates or between PHHs from different individuals was compared (Figure S10; data in Excel Table S20). The average percentage of coefficient of variation within a gene was three to four times higher between different PHHs (intersubject intra-gene variability, blue bars) than between replicates (intra-subject-gene variability, red bars) depending on the compound and time point.

To further assess differences in PHH sensitivity, sensitivity scores were determined based on both the median BMC and maxFC for the top 50 responsive genes for each compound for both time points ([Figure 3B](#); Figure S8; Excel Table S6). A subset of PHHs (cluster I–II) showed high sensitivity scores for all stress responses induced by the reference compounds and also showed higher cell death induction at the highest concentration of DEM for some of the PHHs within this cluster ([Figure 3B](#)). In addition, a subpanel of PHHs (cluster III) was highly sensitive toward TNFα, while being insensitive toward all other chemical-induced stress responses. Thus, PHHs could be sensitive to chemical compounds in general but also selectively sensitive for specific types of stress-inducing chemicals. In addition, a positive Pearson's correlation of 0.27 (with $p < 0.1$) could be observed between cell death induction as measured by LDH leakage and the sensitivity scores for DEM, where a subset of PHHs with high LDH leakage were more sensitive for DEM-mediated stress response activation ([Figure 3B](#); Figure S11).

Next, we calculated a data-driven toxicodynamic variability factor ($TDVF_{0.01}$), which is the ratio between the median population point-of-departure (PoD) and the 1% quantile individual PoD. This $TDVF_{0.01}$ accounts for underestimation of the variance within the human population when estimating the PoDs for cellular stress response activation upon chemical exposures ([Table 1](#)). For DEM-mediated oxidative stress and CPT-induced DNA damage, the commonly used toxicodynamic UF[9] of 3.16 would be enough since data-based $TDVF_{0.01}$ values were all lower at both the 8- and 24-h time points. However, for 8-h TUN-induced UPR activation and TNFα-mediated NF-κB signaling, the defined $TDVF_{0.01}$ was higher than the UF of 3.16, namely 6.5 and 26.5, respectively. At the 24-h time point, TUN-induced UPR had a $TDVF_{0.01}$ of 5, which is also higher than the standard UF.

Influence of Pathology on Stress Response Activation

Interindividual variability could be based on liver pathology background of donors. Therefore, next, the influence of the disease status, such as cancer or different types of liver pathology, on stress response activation upon chemical exposure in PHHs was evaluated. In general, the presence of cancer in any tissue type (Excel Table S1) did

Table 1. Median benchmark concentrations (BMC) for each primary human hepatocytes (PHH) based on top 50 stress responsive genes for each compound and time point.

Time point	CMP	Median BMC ± SD[a] (minimum–maximum)	Fold change min-max median BMC	$TDVF_{0.01}$[b] (exp data)	$TDVF_{0.01}$ (model)[c]	SD $TDVF_{0.01}$ (model)[c]
8 h	TUN	0.534 ± 1.320 μM (0.009–7.768)	864.1	6.545	6.317	0.582
	DEM	352.486 ± 243.643 μM (111.726–1,405.220)	12.6	2.517	1.828	0.066
	CPT	9.488 ± 5.867 μM (2.640–35.447)	13.4	2.786	3.241	0.202
	TNF	12.447 ± 13.310 ng/mL (0.157–40.633)	258.8	26.524	5.315	0.423
24 h	TUN	0.023 ± 0.061 μM (0.002–0.447)	223.5	4.950	4.811	0.386
	DEM	315.597 ± 108.883 μM (176.656–623.096)	3.5	1.701	1.624	0.047
	CPT	3.083 ± 1.022 μM (1.471–6.401)	4.4	1.847	2.184	0.090
	TNF	0.926 ± 2.252 ng/mL (0.137–15.263)	111.4	2.516	2.556	0.128

Note: BMC, benchmark concentration; CMP, compound; CPT, cisplatin; DEM, diethyl maleate; exp, experimental; PHH, primary human hepatocytes; SD, standard deviation; TDVF, toxicodynamic variability factor; TNFα, tumor necrosis factor alpha; TUN, tunicamycin.
[a]The mean ± SD of the median BMC of the top 50 stress responsive genes across the PHH panel.
[b]$TDVF_{0.01}$ is the ratio between the median BMC of the panel and the 1% quantile individual BMC.
[c]Based on population modeling of 2,000 virtual donors for 1,000 assays.

not have an obvious influence on the sensitivity of the PHHs toward chemical-induced stress, since clear clustering of sensitivity scores of PHHs derived from patients with cancer was not observed (Figure 3B). In addition, presence of cancer only mildly influenced the distribution of median maxFC and BMC for the top 50 stress responsive genes (Figure S12A,B). In contrast, PHHs from patients having any type of liver pathology including liver cancer (Excel Table S1) were in general less sensitive toward chemical-induced stress with regard to transcriptomic changes, especially for TUN-induced UPR and TNFα-induced NF-κB signaling (Figure 3B). When we evaluated the distribution of the median maxFC, a significant difference could be observed between PHHs derived from patients with or without liver pathology when exposed to TUN or TNFα for 24 h (Figure 3C). The same trend was observed for DEM and CPT, although this was not significant. Possibly, PHHs from patients with a certain liver pathology were already at a higher level of stress leading to lower fold changes upon chemical-induced stress. Indeed, these PHHs showed in general significant slightly higher basal expression of the top 50 stress responsive genes compared to PHHs without liver pathology (Figure S12C; Excel Table S4). Variability in differentiation status did not have an effect on BMC and maxFC distribution (Figure S13; data in Excel Table S21).

Variability in Pathway Enrichment upon Chemical Exposure

To obtain more insight into chemical-induced stress pathway activation, gene set enrichment analysis of gene ontology terms was performed using the maxFC as input for ranking of the genes. In general, upon exposure to each reference compound, expected terms were enriched related to anticipated chemical-induced stress response pathways (Figure 4A; Figure S14). For instance, TUN treatment led to the strong enrichment of ER stress and UPR-related terms, TNFα resulted in chemotaxis and chemokine-related terms, DEM gave enrichment of heat shock or ion response-related terms, and CPT treatment led to enrichment of ion or metabolic-related terms compared to solvent control. All chemicals led to enrichment for both sensitive and insensitive PHHs, although some terms were more specific for either sensitive or insensitive PHHs, e.g., terms related to response to ions were more enriched for insensitive PHHs upon DEM exposure (Figure 4A). Clustering of enriched terms for at least three PHHs showed specific enrichment of terms related to ribosomal localization or subunits for insensitive PHHs upon TUN or CPT exposure, while terms related to response to virus or interferon were enriched for specifically sensitive PHHs upon TNFα treatment (Figure 4B).

Interindividual Variability in Stress Response Activation by Hepatotoxicants

The interindividual difference in sensitivity toward chemical-induced oxidative stress response and UPR activation was further analyzed by screening the three most sensitive and insensitive PHHs based on the sensitivity score with various hepatotoxicants known to induce oxidative stress (acetaminophen, propylthiouracyl, and nitrofurantoin) or ER stress (ticlopidine, nefazodone, and diclofenac) (Figure 5). Upon evaluation of differences in cell death induction, a concentration-dependent increase in LDH leakage was observed for all tested hepatotoxicants, except for acetaminophen and propylthiouracil (Figure 5A). Both nitrofurantoin and nefazodone already showed cell death induction at 25× Cmax or higher. Two out of the three most sensitive PHHs showed higher cytotoxicity when exposed to nitrofurantoin and diclofenac than the most insensitive PHHs. For the other hepatotoxicants, no difference was observed. Next, the expression of the top 50 responsive genes identified earlier was evaluated for both

the oxidative stress response and UPR, where in particular nitrofurantoin showed higher induction in sensitive PHHs compared to two out of the three insensitive PHHs (Figure 5B). Other hepatotoxicants did not show clear distinction when only evaluating these genes. Thereafter, the difference in the distribution of BMCs and maxFC of all responsive genes was evaluated between the most sensitive and insensitive PHHs for each tested hepatotoxicant. The hepatotoxicants propylthiouracyl and acetaminophen showed separation between the sensitive and two out of three insensitive PHHs in BMC and maxFC distribution (Figure 5C; Tables 2 and 3). In contrast, one of the insensitive PHHs had lower BMCs compared to all sensitive PHHs for these hepatotoxicants. For all other hepatotoxicants, differences in BMCs and maxFCs between PHHs were variable.

Influence of PHH Panel Size on Estimated BMC and maxFC CVs

To check the interindividual variability model for the entire human population in chemical-induced stress response activation, both the BMC and maxFC for the top 50 stress responsive genes for each compound was simulated for 500 virtual PHHs. The distribution of the simulated BMCs and maxFCs were in concordance with the experimental data based on the panel of 50 PHHs showing similar distributions (Figure S15 and S16).

Larger-scale predictive simulations (of 1,000 simulated panels of various sizes) were used to obtain distributions of BMC and maxFC CV values for the top 50 stress responsive genes for each reference compound (Figure 6A,B). When the PHH panel size was increased, the CV estimates became increasingly precise and converge to the estimated large-sample human population variability. For small PHH panel sizes, which are commonly used during hepatotoxicity testing, the imprecision was very large, leading to consistent underestimation of the interindividual variance in stress response activation upon chemical exposure.

Next, the probability of obtaining a CV, which is close to the estimated large-sample human population CV, was evaluated when using different PHH panel sizes (Figure 6C,D). Overall, when using a PHH panel size of 10 or less, the probability to estimate the correct CV of the BMC was very low, namely smaller than ~ 0.3, 0.05, 0.15, and 0.2 for DEM, CPT, TUN, and TNFα, respectively (Figure 6C). When using a PHH panel size of 50, the maximal probability that could be reached to estimate the correct CV of the BMC was ~ 0.45, 0.3, 0.4, and 0.4 for DEM, CPT, TUN, and TNFα, respectively, still resulting in quite some uncertainty. For estimating the correct CV of the maxFC, a maximal probability of 0.3 was reached for all compounds when using a PHH panel size of 50, which was also still quite low (Figure 6D). Therefore, an additional uncertainty factor might be needed to cover the uncertainty in estimating the true median population PoD and all of the variance of stress response activation upon chemical exposure during hepatotoxicity testing in PHHs. Indeed, simulation of 2,000 virtual donors for 1,000 assays resulted in $TDVF_{0.01}$ values that were up to 2-fold higher than the standard used UF of 3.16 for TUN, CPT, and TNFα for 8 h and TUN for 24 h (Table 1).

Discussion

Human tissue-culture-based methods hold great promise for the prediction of chemical-induced adversities.[59–61] Here, we evaluated the effects of interindividual differences in sensitivity to chemical-induced stress in PHHs to determine data-driven toxicodynamic UFs for specific types of relevant stress responses that are critical in chemical-induced toxicity. In our analysis, we focused on chemicals inducing the UPR, the oxidative stress
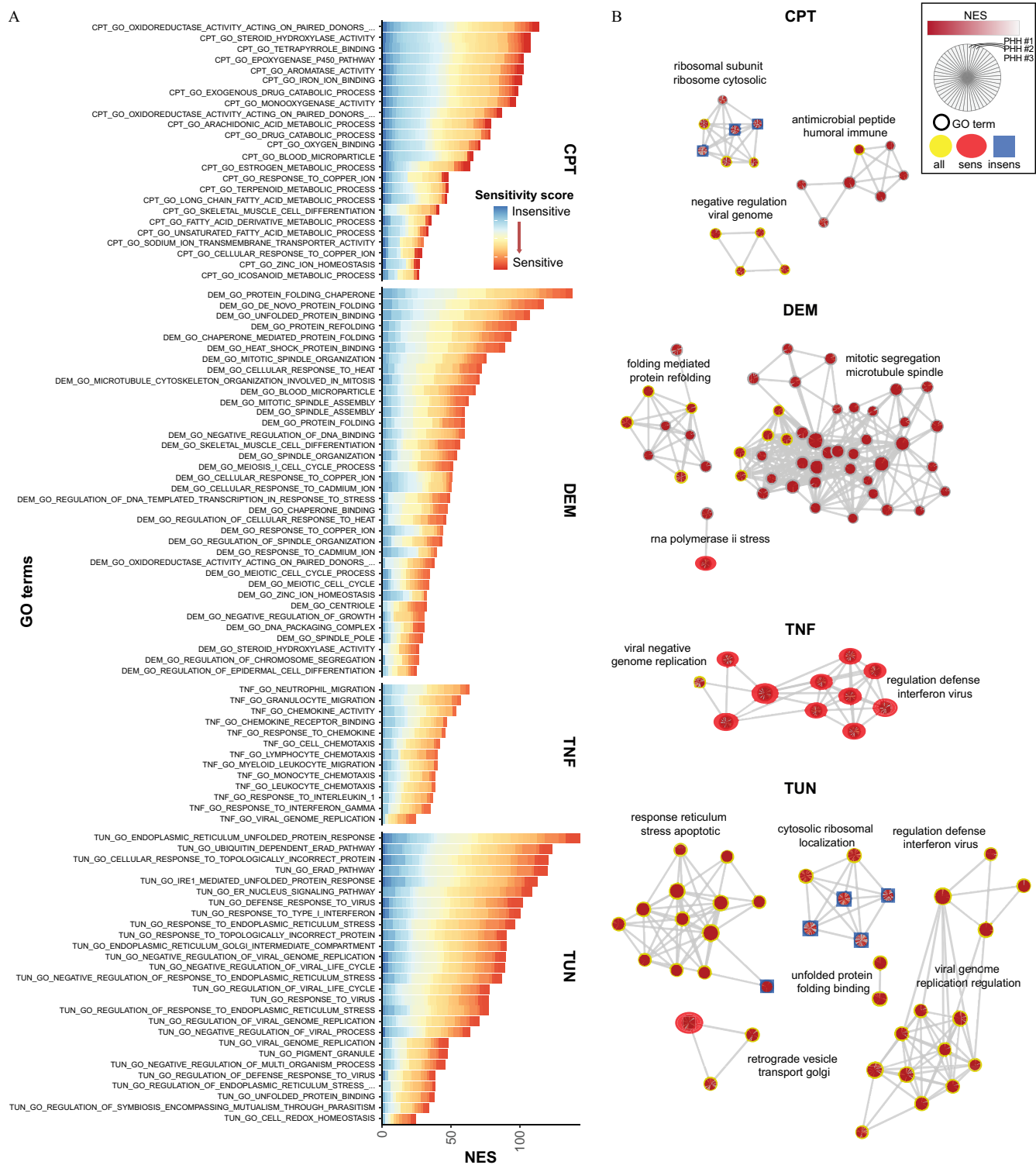
Figure 4. Variability in gene set enrichment upon chemical-induced stress. Gene set enrichment analysis[33] was done using gene ontology terms version 7.1 and the maximal fold change across concentration range (maxFC) compared to solvent control of measured S1500+ gene set of NIEHS[41] supplemented with additional stress response-relevant genes (Excel Table S2) as input for each primary human hepatocytes (PHH) and treatment for 24 h with each reference compound; diethyl maleate (DEM), tunicamycin (TUN), cisplatin (CPT), and TNF (TNFα). (A) Bar plots of normalized enrichment scores (NES) of significantly enriched gene ontology (GO) terms with a cut-off of adjusted false discovery rate (FDR) of <0.05 for at least 10 different PHHs. NES were stacked for all PHHs showing significant enrichment for each term. (B) Clusters of significantly enriched GO terms showing specific enrichment in either most sensitive (red eclipse) or insensitive (blue square) PHHs, or in both (yellow circle) for one of the terms within the cluster using Cytoscape[55] and EnrichmentMap.[56] PHHs were classified as most sensitive or insensitive having a sensitivity score lower than the first quartile or higher than the third quartile of the sensitivity scores for all PHHs, respectively. Sensitivity scores were determined based on both the median BMC and maxFC for the top 50 responsive genes for each compound for both time points. Within each term, NES for each PHH is depicted in gray to red scale from low to high. Enriched GO terms were clustered and summarized with three to four keywords using WordCloud.[57] Edges between nodes were based on similarity between gene sets with a similarity cut-off of 0.375. Data shown is reported in Excel Table S7 and S10. Note: NIEHS, National Institute of Environmental Health Sciences; TNFα, tumor necrosis factor alpha.
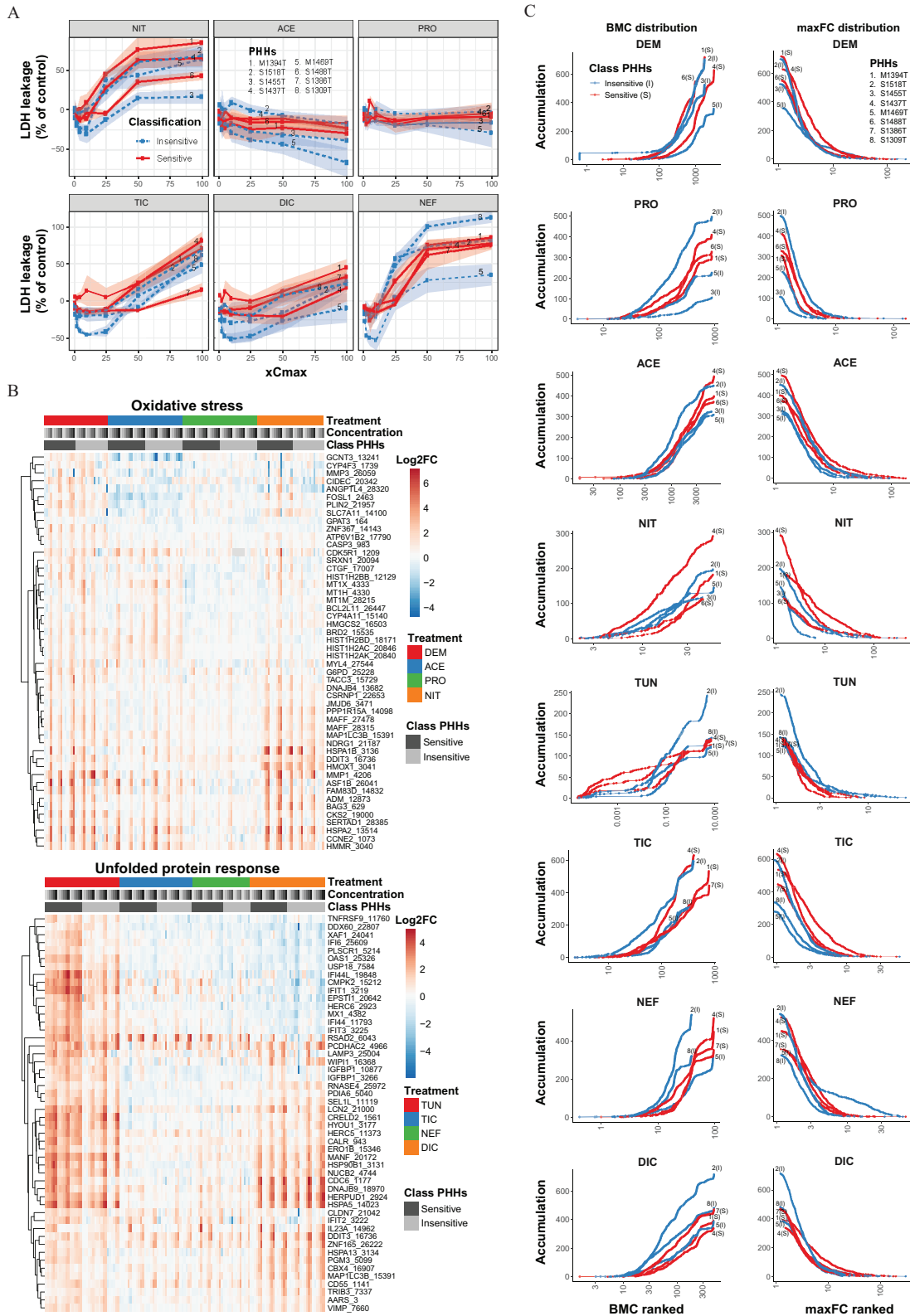
Figure 5. Difference in sensitivity toward hepatotoxicants within a subpanel of primary human hepatocytes (PHHs). (A) LDH leakage upon treatment with hepatotoxicants for 24 h in six defined most sensitive or insensitive PHHs. (B) Hierarchical clustering of log2 fold changes compared to solvent control of top 50 stress responsive genes [identified based on diethyl maleate (DEM) for oxidative stress or tunicamycin (TUN) for unfolded protein response treatment mostly strongly induced at the lowest effective concentration] of PHHs exposed to various hepatotoxicants for 24 h. (C) Distribution of benchmark concentration (BMC) in µM and maximal fold change across concentration range (maxFC) for all responsive genes of PHHs exposed to various hepatotoxicants for 24 h. Data shown is reported in Excel Table S11 and S12. $n = 3$. Note: ACE, acetaminophen; DIC, diclofenac; LDH, lactate dehydrogenase; NEF, nefazodone; NIT, nitrofurantoin; PRO, propylthiouracil; TIC, ticlopidine.

Table 2. Median benchmark concentration (BMC) for most sensitive and insensitive primary human hepatocytes (PHHs) based on all responsive genes for each treatment.

CMP	Insensitive PHHs			Sensitive PHHs		
OX	M1469T	S1455T	S1518T	M1394T	S1437T	S1488T
DEM	1,024.47	580.07	629.48	672.95	1,051.43	375.30 μM
ACE	1,528.25	1,331.12	1,069.92	1,761.77	1,993.41	1,379.58 μM
NIT	20.65	11.60	24.03	29.02	17.37	22.12 μM
PRO	293.33	345.93	193.57	312.23	311.24	235.90 μM
UPR	M1469T	S1309T	S1518T	M1394T	S1386T	S1437T
TUN	0.07	0.21	0.19	0.004	0.19	0.04 μM
DIC	122.25	72.45	68.45	137.28	99.12	137.80 μM
NEF	37.31	18.24	19.01	37.25	25.66	40.28 μM
TIC	103.17	141.57	96.00	229.69	210.65	151.71 μM

Note: ACE, acetaminophen; CMP, compound; DEM, diethyl maleate; DIC, diclofenac; NEF, nefazodone; NIT, nitrofurantoin; OX, oxidative stress response; PRO, propylthiouracil; TIC, ticlopidine; TUN, tunicamycin; UPR, unfolded protein response.

response, the DNA damage response, and cytokine-mediated NF-κB signaling. The activation of each of these stress responses is considered a key event leading to the development of chemical-induced liver injury.[62] Moreover, the consequent upregulation of a specific set of gene transcripts that represents these stress response pathways can be used to qualify and quantify the mode-of-action for the evaluation of hepatotoxicity.[31,63] Our results indicated that large differences in the distribution of BMCs were observed between different PHHs exposed to specific stress response inducers. This work indicates that the standard UF for toxicodynamic responses for risk assessment might not be sufficient for toxicity responses that would involve in particular UPR and NF-κB signaling. Evaluating the suitability of the estimated data-driven UFs in this study for other hepatotoxic-inducing chemicals and how this translates to the human liver *in vivo* is important. Potentially, additional chemical-specific together with end point-specific UFs are needed.

Our data indicates the need of accurately determined data-driven UFs during risk assessment to improve the prediction of liabilities for chemical-induced liver injury. Our results indicated that these UFs based on stress response activation in plated cryopreserved PHHs could be at least 2-fold higher than the standard toxicodynamic UF of 3.16. In concordance, Blanchette et al. characterized the human population variance of chemical-induced cardiotoxicity using human induced pluripotent stem cell (hiPSC)-derived cardiomyocyte panel together with population modeling and also showed higher TDVFs than the standard 3.16.[20,38] Likewise, Abdo et al. found that some of the 179 screened chemicals led to TDVF values higher than 10 when evaluating cytotoxicity in 1,086 lymphoblastoid cell lines.[18] Here, the estimated UFs were based on the total variability, taking together variability

Table 3. Median maximal fold change compared to solvent control across concentration range (maxFC) for most sensitive and insensitive primary human hepatocytes (PHHs) based on all responsive genes for each treatment.

CMP	Insensitive PHHs			Sensitive PHHs		
OX	M1469T	S1455T	S1518T	M1394T	S1437T	S1488T
DEM	2.94	2.51	2.25	2.33	3.48	2.53
ACE	3.14	2.95	3.59	2.93	3.61	3.68
NIT	1.92	3.10	3.17	6.31	2.86	3.80
PRO	1.96	1.54	2.16	1.78	2.03	2.22
UPR	M1469T	S1309T	S1518T	M1394T	S1386T	S1437T
TUN	1.84	1.98	1.78	1.73	1.89	1.78
DIC	3.08	2.68	2.88	5.02	2.90	3.70
NEF	3.33	2.13	2.09	2.92	2.61	2.42
TIC	1.97	2.20	2.21	3.63	2.67	2.48

Note: ACE, acetaminophen; CMP, compound; DEM, diethyl maleate; DIC, diclofenac; NEF, nefazodone; NIT, nitrofurantoin; OX, oxidative stress response; PRO, propylthiouracyl; TIC, ticlopidine; TUN, tunicamycin; UPR, unfolded protein response.

between different PHHs (inter-) and between biological replicates (intraindividual variability), the latter being limited. To accurately define UFs, it is important to characterize the difference between intra- and interindividual variability. Other additional technical variabilities that might be of influence on the sensitivity of the PHHs toward chemical exposure is the isolation procedure and difference in dedifferentiation rate. Ischemia time during surgery impacts viability of isolated hepatocytes from liver resections and may add an additional layer of variability.[64] Furthermore, PHHs were cultured in 2D, known to dedifferentiate fast over time, where the dedifferentiation rate can vary between different PHHs. However, since only short-term exposure durations up to 24 h were evaluated, this culture setup was found to be sufficient. Besides, we have selected chemicals that did not need metabolism to induce toxicity and therefore were not affected due to difference in metabolic capacity. However, most optimally, to minimize these technical variabilities and retain variability that exists *in vivo*, cells directly retrieved from different individuals should be used with minimal manipulation and handling, which for PHHs obviously is very challenging.

Potentially, several factors may influence PHH sensitivity to chemical-induced stress, including differences in health characteristics of PHH donors. We found that PHHs from patients with any type of liver disease, including liver cancer, showed less induction of stress responses upon exposure, especially for TNFα-induced NF-κB signaling and TUN-induced UPR. These PHHs showed already higher expression of stress response-related genes in control conditions, thereby leading to less capacity to further induce protective stress responses upon chemical exposure. Indeed, there are strong correlations between liver diseases, such as nonalcoholic fatty liver disease, nonalcoholic steatohepatitis, and liver cancer; increased activation of, e.g., the UPR and the inflammatory response;[63,65–67] and increased liver injury susceptibility.[68,69] Thus, the liver disease background of PHHs can have a significant impact on their sensitivity to hepatotoxicants. In this respect, special attention should be given to the inflammatory state of the liver prior to the isolation of PHHs. Large differences were observed in basal expression of chemokines, such as *CCL2*, possibly affecting their sensitivity toward chemical exposure. Indeed, the presence of inflammation is one of the susceptibility factors for development of liver injury.[70,71] In addition, large variability was also seen in the expression of inflammatory genes upon chemical exposure across a panel of PHHs upon PCA. Inflammatory genes such as *IL1B* and *CCL3* were most differently expressed across the panel of PHHs upon TUN treatment. Several studies have shown the relation between UPR activation and inflammatory signaling through activation of NF-κB and the NLRP3 inflammasome, leading to induction of *IL1B* expression.[72]

In conclusion, we demonstrated that chemical-induced liver injury-associated stress response activation determined by high-throughput transcriptomics is highly variable between plated cryopreserved PHHs derived from different individuals. This highlights the need to use toxicodynamic UFs for safety evaluation. We showed that the currently used standard UF of 3.16 may not be sufficient to capture all gene activation variability for every chemical or end point measured in PHHs. For activation of the UPR and NF-κB signaling, the defined TDVF was up to 2-fold higher than the standard UF. This exemplifies a general need for the definition of data-driven mechanism-specific UFs to accurately correct for toxicodynamic variability across the human population to improve assessment of liabilities for development of liver injury by environmental toxicants or drugs. Whether similar interindividual variability is observed *in vivo* or in other target organ systems as well as other critical toxicity related pathways requires further systematic studies.
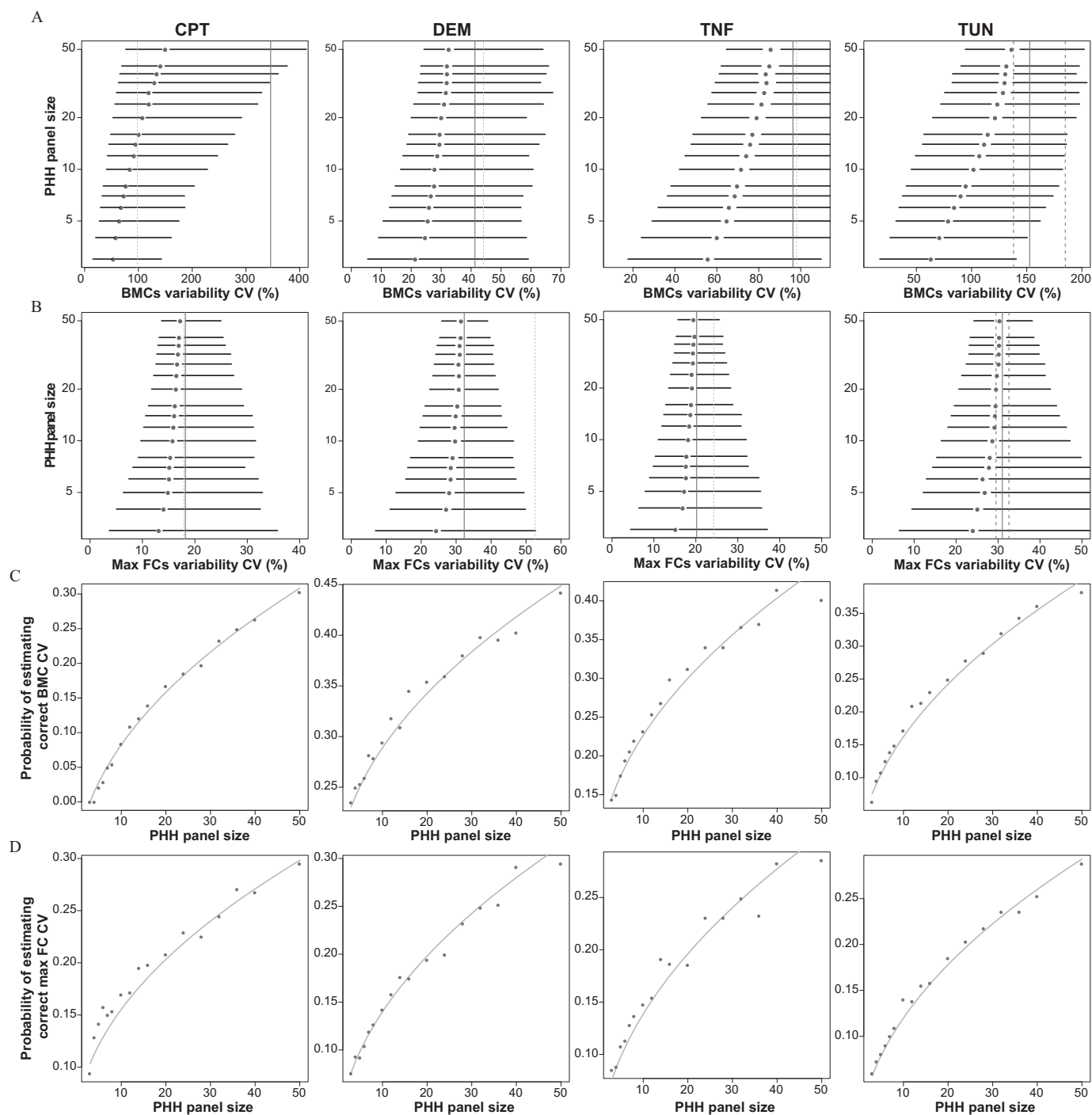
Figure 6. Influence of primary human hepatocyte (PHH) panel size on probability to capture correct variance in stress response activation. (A,B) Forest plots of simulated distributions (medians ± 5th/95th percentiles) of the estimated coefficients of variation (CVs) of benchmark concentrations (BMC) (A) and maximal fold changes across concentration range (maxFC) compared to solvent control (B) based on top 50 stress responsive genes for each reference compound [diethyl maleate (DEM), tunicamycin (TUN), cisplatin (CPT), and TNF (TNFα)] as a function of PHH panel size. As reference, 1,000 assays with a panel of PHHs from 2,000 individuals was simulated depicted as lines (median: solid ± 5th/95th percentiles: dashed). (C,D) Probability of reporting a correct CV falling between the 5th and 95th percentile of the reference CVs as a function of PHH panel size for BMC (C) and maxFC (D). Dots resemble Monte Carlo simulation estimates and lines resemble visually fitted smoothing curves. Data shown is reported in Excel Tables S13 and S14. Note: TNFα, tumor necrosis factor alpha.

References

1. Olson H, Betton G, Robinson D, Thomas K, Monro A, Kolaja G, et al. 2000. Concordance of the toxicity of pharmaceuticals in humans and in animals. Regul Toxicol Pharmacol 32(1):56–67, PMID: 11029269, https://doi.org/10.1006/rtph.2000.1399.

2. Watkins PB. 2011. Drug safety sciences and the bottleneck in drug development. Clin Pharmacol Ther 89(6):788–790, PMID: 21593756, https://doi.org/10.1038/clpt.2011.63.

3. Sen P, Qadri S, Luukkonen PK, Ragnarsdottir O, McGlinchey A, Jäntti S, et al. 2022. Exposure to environmental contaminants is associated with altered hepatic lipid metabolism in non-alcoholic fatty liver disease. J Hepatol 76(2):283–293, PMID: 34627976, https://doi.org/10.1016/j.jhep.2021.09.039.

4. Melaram R. 2021. Environmental risk factors implicated in liver disease: a mini-review. Front Public Health 9:683719, PMID: 34249849, https://doi.org/10.3389/fpubh.2021.683719.

5. Schnegelberger RD, Lang AL, Arteel GE, Beier JI. 2021. Environmental toxicant-induced maladaptive mitochondrial changes: a potential unifying mechanism in fatty liver disease? Acta Pharm Sin B 11(12):3756–3767, PMID: 35024304, https://doi.org/10.1016/j.apsb.2021.09.002.

6. Kullak-Ublick GA, Andrade RJ, Merz M, End P, Benesic A, Gerbes AL, et al. 2017. Drug-induced liver injury: recent advances in diagnosis and risk assessment. Gut 66(6):1154–1164, PMID: 28341748, https://doi.org/10.1136/gutjnl-2016-313369.

7. Gómez-Lechón MJ, Tolosa L, Conde I, Teresa M. 2014. Competency of different cell models to predict human hepatotoxic drugs. Expert Opin Drug Metab Toxicol 10(11):1553–1568, PMID: 25297626, https://doi.org/10.1517/17425255.2014.967680.

8. Gupta R, Schrooders Y, Hauser D, van Herwijnen M, Albrecht W, Ter Braak B, et al. 2021. Comparing in vitro human liver models to in vivo human liver using RNA-Seq. Arch Toxicol 95(2):573–589, PMID: 33106934, https://doi.org/10.1007/s00204-020-02937-6.

9. WHO (World Health Organization). 2005. *Chemical-Specific Adjustment Factors for Interspecies Differences and Human Variability: Guidance Document for Use of Data in Dose/Concentration-Response Assessment. IPCS* Harmonization Project Document No. 2. Geneva, Switzerland: WHO.

10. Vettorazzi G. 1977. Safety factors and their application in the toxicological evaluation. In: *The Evaluation of Toxicological Data for the Protection of Public Health*. December 1976. Oxford, UK: Pergamon Press, 207–223.

11. Dourson ML, Stara JF. 1983. Regulatory history and experimental support of uncertainty (safety) factors. Regul Toxicol Pharmacol 3(3):224–238, PMID: 6356243, https://doi.org/10.1016/0273-2300(83)90030-2.

12. Burin GJ, Saunders DR. 1999. Addressing human variability in risk assessment—the robustness of the intraspecies uncertainty factor. Regul Toxicol Pharmacol 30(3):209–216, PMID: 10620470, https://doi.org/10.1006/rtph.1999.1351.

13. Dorne JLCM. 2004. Impact of inter-individual differences in drug metabolism and pharmacokinetics on safety evaluation. Fundam Clin Pharmacol 18(6):609–620, PMID: 15548231, https://doi.org/10.1111/j.1472-8206.2004.00292.x.

14. Bois FY, Jamei M, Clewell HJ. 2010. PBPK modelling of inter-individual variability in the pharmacokinetics of environmental chemicals. Toxicology 278(3):256–267, PMID: 20600548, https://doi.org/10.1016/j.tox.2010.06.007.

15. Wedagedera JR, Afuape A, Chirumamilla SK, Momiji H, Leary R, Dunlavey M, et al. 2022. Population PBPK modeling using parametric and nonparametric methods of the simcyp simulator, and bayesian samplers. CPT Pharmacometrics Syst Pharmacol 11(6):755–765, PMID: 35385609, https://doi.org/10.1002/psp4.12787.

16. Krauss M, Burghaus R, Lippert J, Niemi M, Neuvonen P, Schuppert A, et al. 2013. Using Bayesian-PBPK modeling for assessment of inter-individual variability and subgroup stratification. In Silico Pharmacol 1:6, PMID: 25505651, https://doi.org/10.1186/2193-9616-1-6.

17. den Braver-Sewradj SP, den Braver MW, van Dijk M, Zhang Y, Dekker SJ, Wijaya L, et al. 2018. Inter-individual variability in activity of the major drug metabolizing enzymes in liver homogenates of 20 individuals. Curr Drug Metab 19(4):370–381, PMID: 29318967, https://doi.org/10.2174/1389200219666180108160046.

18. Abdo N, Xia M, Brown CC, Kosyk O, Huang R, Sakamuru S, et al. 2015. Population-based in vitro hazard and concentration-response assessment of chemicals: the 1000 genomes high-throughput screening study. Environ Health Perspect 123(5):458–466, PMID: 25622337, https://doi.org/10.1289/ehp.1408775.

19. Chiu WA, Wright FA, Rusyn I. 2017. A tiered, Bayesian approach to estimating population variability for regulatory decision-making. ALTEX 34(3):377–388, PMID: 27960008, https://doi.org/10.14573/altex.1608251.

20. Blanchette AD, Burnett SD, Grimm FA, Rusyn I, Chiu WA. 2020. A Bayesian method for population-wide cardiotoxicity hazard and risk characterization using an in vitro human model. Toxicol Sci 178(2):391–403, PMID: 33078833, https://doi.org/10.1093/toxsci/kfaa151.

21. Copple IM, den Hollander W, Callegaro G, Mutter FE, Maggs JL, Schofield AL, et al. 2019. Characterisation of the NRF2 transcriptional network and its response to chemical insult in primary human hepatocytes: implications for prediction of drug-induced liver injury. Arch Toxicol 93(2):385–399, PMID: 30426165, https://doi.org/10.1007/s00204-018-2354-1.

22. Ramachandran A, Jaeschke H. 2018. Oxidative stress and acute hepatic injury. Curr Opin Toxicol 7:17–21, PMID: 29399645, https://doi.org/10.1016/j.cotox.2017.10.011.

23. Burban A, Sharanek A, Guguen-Guillouzo C, Guillouzo A. 2018. Endoplasmic reticulum stress precedes oxidative stress in antibiotic-induced cholestasis and cytotoxicity in human hepatocytes. Free Radic Biol Med 115:166–178, PMID: 29191461, https://doi.org/10.1016/j.freeradbiomed.2017.11.017.

24. Fredriksson L, Wink S, Herpers B, Benedetti G, Hadi M, de Bont H, et al. 2014. Drug-induced endoplasmic reticulum and oxidative stress responses independently sensitize toward TNFα-mediated hepatotoxicity. Toxicol Sci 140(1):144–159, PMID: 24752500, https://doi.org/10.1093/toxsci/kfu072.

25. Lafleur MA, Stevens JL, Lawrence JW. 2013. Xenobiotic perturbation of ER stress and the unfolded protein response. Toxicol Pathol 41(2):235–262, PMID: 23334697, https://doi.org/10.1177/0192623312470764.

26. Hartwig A, Arand M, Epe B, Guth S, Jahnke G, Lampen A, et al. 2020. Mode of action-based risk assessment of genotoxic carcinogens. Arch Toxicol 94(6):1787–1877, PMID: 32542409, https://doi.org/10.1007/s00204-020-02733-2.

27. Hanson RL, Porter JR, Batchelor E. 2019. Protein stability of p53 targets determines their temporal expression dynamics in response to p53 pulsing. J Cell Biol 218(4):1282–1297, PMID: 30745421, https://doi.org/10.1083/jcb.201803063.

28. Hafner A, Bulyk ML, Jambhekar A, Lahav G. 2019. The multiple mechanisms that regulate p53 activity and cell fate. Nat Rev Mol Cell Biol 20(4):199–210, PMID: 30824861, https://doi.org/10.1038/s41580-019-0110-x.

29. Fredriksson L, Herpers B, Benedetti G, Matadin Q, Puigvert JC, de Bont H, et al. 2011. Diclofenac inhibits tumor necrosis factor-α-induced nuclear factor-κB activation causing synergistic hepatocyte apoptosis. Hepatology 53(6):2027–2041, PMID: 21433042, https://doi.org/10.1002/hep.24314.

30. Beggs KM, Maiuri AR, Fullerton AM, Poulsen KL, Breier AB, Ganey PE, et al. 2015. Trovafloxacin-induced replication stress sensitizes HepG2 cells to tumor necrosis factor-alpha-induced cytotoxicity mediated by extracellular signal-regulated kinase and ataxia telangiectasia and Rad3-related. Toxicology 331:35–46, PMID: 25748550, https://doi.org/10.1016/j.tox.2015.03.002.

31. Wink S, Hiemstra SW, Huppelschoten S, Klip JE, van de Water B. 2018. Dynamic imaging of adaptive stress response pathway activation for prediction of drug induced liver injury. Arch Toxicol 92(5):1797–1814, https://doi.org/10.1007/s00204-018-2178-z.

32. Wink S, Hiemstra S, Herpers B, van de Water B. 2017. High-content imaging-based BAC-GFP toxicity pathway reporters to assess chemical adversity liabilities. Arch Toxicol 91(3):1367–1383, PMID: 27358234, https://doi.org/10.1007/s00204-016-1781-0.

33. Jennings P. 2013. Stress response pathways, toxicity pathways and adverse outcome pathways. Arch Toxicol 87(1):13–14, PMID: 23149676, https://doi.org/10.1007/s00204-012-0974-4.

34. Ter Braak B, Niemeijer M, Boon R, Parmentier C, Baze A, Richert L, et al. 2021. Systematic transcriptome-based comparison of cellular adaptive stress response activation networks in hepatic stem cell-derived progeny and primary human hepatocytes. Toxicol In Vitro 73:105107, PMID: 33545341, https://doi.org/10.1016/j.tiv.2021.105107.

35. Godoy P, Schmidt-Heck W, Natarajan K, Lucendo-Villarin B, Szkolnicka D, Asplund A, et al. 2015. Gene networks and transcription factor motifs defining the differentiation of stem cells into hepatocyte-like cells. J Hepatol 63(4):934–942, PMID: 26022688, https://doi.org/10.1016/j.jhep.2015.05.013.

36. Yeakley JM, Shepard PJ, Goyena DE, Vansteenhouse HC, McComb JD, Seligmann BE. 2017. A trichostatin a expression signature identified by TempO-seq targeted whole transcriptome profiling. PLoS One 12(5):e0178302, PMID: 28542535, https://doi.org/10.1371/journal.pone.0178302.

37. Hiemstra S, Ramaiahgari SC, Wink S, Callegaro G, Coonen M, Meerman J, et al. 2019. High-throughput confocal imaging of differentiated 3D liver-like spheroid cellular stress response reporters for identification of drug-induced liver injury liability. Arch Toxicol 93(10):2895–2911, PMID: 31552476, https://doi.org/10.1007/s00204-019-02552-0.

38. Burnett SD, Blanchette AD, Grimm FA, House JS, Reif DM, Wright FA, et al. 2019. Population-based toxicity screening in human induced pluripotent stem cell-derived cardiomyocytes. Toxicol Appl Pharmacol 381:114711, PMID: 31425687, https://doi.org/10.1016/j.taap.2019.114711.

39. Alexandre E, Baze A, Parmentier C, Desbans C, Pekthong D, Gerin B, et al. 2012. Plateable cryopreserved human hepatocytes for the assessment of cytochrome P450 inducibility: experimental condition-related variables affecting their response to inducers. Xenobiotica 42(10):968–979, PMID: 22515431, https://doi.org/10.3109/00498254.2012.676693.

40. Strober W. 2001. Trypan blue exclusion test of cell viability. Curr Protoc Immunol Appendix 3:Appendix 3B, PMID: 18432654, https://doi.org/10.1002/0471142735.ima03bs21.

41. Mav D, Shah RR, Howard BE, Auerbach SS, Bushel PR, Collins JB, et al. 2018. A hybrid gene selection approach to create the S1500+ targeted gene sets for use in high-throughput transcriptomics. PLoS One 13(2):e0191105, https://doi.org/10.1371/journal.pone.0191105.

42. Love MI, Huber W, Anders S. 2014. Moderated estimation of fold change and dispersion for RNA-seq data with DESeq2. Genome Biol 15(12):550, https://doi.org/10.1186/s13059-014-0550-8.

43. Yang L, Allen BC, Thomas RS. 2007. BMDExpress: a software tool for the benchmark dose analyses of genomic data. BMC Genomics 8(1):387, https://doi.org/10.1186/1471-2164-8-387.

44. Phillips JR, Svoboda DL, Tandon A, Patel S, Sedykh A, Mav D, et al. 2019. BMD express 2: enhanced transcriptomic dose-response analysis workflow. Bioinformatics 35(10):1780–1782, PMID: 30329029, https://doi.org/10.1093/bioinformatics/bty878.

45. Thomas PD, Ebert D, Muruganujan A, Mushayahama T, Albou LP, Mi H. 2022. PANTHER: making genome-scale phylogenetics accessible to all. Protein Sci 31(1):8–22, PMID: 34717010, https://doi.org/10.1002/pro.4218.

46. Mi H, Muruganujan A, Huang X, Ebert D, Mills C, Guo X, et al. 2019. Protocol update for large-scale genome and gene function analysis with the PANTHER classification system (v.14.0). Nat Protoc 14(3):703–721, PMID: 30804569, https://doi.org/10.1038/s41596-019-0128-8.

47. Kolde R. 2019. pheatmap: pretty heatmaps. R package version 1.0.12. https://CRAN.R-project.org/package=pheatmap [accessed 4 January 2019].

48. Wickham H. 2016. *ggplot2: Elegant Graphics for Data Analysis*. New York, NY: Springer-Verlag.

49. Dowle M, Srinivasan A. 2021. data.table: extension of 'data.framè. R package version 1.14.0. https://CRAN.R-project.org/package=data.table [accessed 21 February 2021].

50. Wickham H, François R, Henry L, Müller K. 2021. dplyr: A Grammar of Data Manipulation. R package version 1.0.5. https://CRAN.R-project.org/package=dplyr [accessed 5 March 2021].

51. Wickham H. 2007. Reshaping data with the reshape package. J Stat Soft 21(12):1–20, https://doi.org/10.18637/jss.v021.i12.

52. Carbon S, Douglass E, Good BM, Unni DR, Harris NL, Mungall CJ, et al. 2021. The gene ontology resource: enriching a GOld mine. Nucleic Acids Res 49(D1):D325–D334, https://doi.org/10.1093/nar/gkaa1113.

53. Subramanian A, Tamayo P, Mootha VK, Mukherjee S, Ebert BL, Gillette MA, et al. 2005. Gene set enrichment analysis: a knowledge-based approach for interpreting genome-wide expression profiles. Proc Natl Acad Sci USA 102(43):15545–15550, PMID: 16199517, https://doi.org/10.1073/pnas.0506580102.

54. Liberzon A, Subramanian A, Pinchback R, Thorvaldsdóttir H, Tamayo P, Mesirov JP. 2011. Molecular signatures database (MSigDB) 3.0. Bioinformatics 27(12):1739–1740, PMID: 21546393, https://doi.org/10.1093/bioinformatics/btr260.

55. Shannon P, Markiel A, Ozier O, Baliga NS, Wang JT, Ramage D, et al. 2003. Cytoscape: a software environment for integrated models of biomolecular interaction networks. Genome Res 13(11):2498–2504, PMID: 14597658, https://doi.org/10.1101/gr.1239303.

56. Merico D, Isserlin R, Stueker O, Emili A, Bader GD. 2010. Enrichment map: a network-based method for gene-set enrichment visualization and interpretation. PLoS One 5(11):e13984, PMID: 21085593, https://doi.org/10.1371/journal.pone.0013984.

57. Oesper L, Merico D, Isserlin R, Bader GD. 2011. WordCloud: a cytoscape plugin to create a visual semantic summary of networks. Source Code Biol Med 6(1):7, https://doi.org/10.1186/1751-0473-6-7.

58. Gelman A. 2006. Prior distributions for variance parameters in hierarchical models (comment on article by browne and draper). Bayesian Anal 1(3):515–534, https://doi.org/10.1214/06-BA117A.

59. Bell CC, Dankers ACA, Lauschke VM, Sison-Young R, Jenkins R, Rowe C, et al. 2018. Comparison of hepatic 2D sandwich cultures and 3D spheroids for long-term toxicity applications: a multicenter study. Toxicol Sci 162(2):655–666, PMID: 29329425, https://doi.org/10.1093/toxsci/kfx289.

60. Tabernilla A, Dos Santos Rodrigues B, Pieters A, Caufriez A, Leroy K, Van Campenhout R, et al. 2021. In vitro liver toxicity testing of chemicals: a pragmatic approach. Int J Mol Sci 22(9):5038, PMID: 34068678, https://doi.org/10.3390/ijms22095038.

61. Shah I, Antonijevic T, Chambers B, Harrill J, Thomas R. 2021. Estimating hepatotoxic doses using high-content imaging in primary hepatocytes. Toxicol Sci 183(2):285–301, PMID: 34289070, https://doi.org/10.1093/toxsci/kfab091.

62. Weaver RJ, Blomme EA, Chadwick AE, Copple IM, Gerets HHJ, Goldring CE, et al. 2020. Managing the challenge of drug-induced liver injury: a roadmap for the development and deployment of preclinical predictive models. Nat Rev Drug Discov 19(2):131–148, PMID: 31748707, https://doi.org/10.1038/s41573-019-0048-x.

63. Lebeaupin C, Vallée D, Hazari Y, Hetz C, Chevet E, Bailly-Maitre B. 2018. Endoplasmic reticulum stress signalling and the pathogenesis of non-alcoholic fatty liver disease. J Hepatol 69(4):927–947, PMID: 29940269, https://doi.org/10.1016/j.jhep.2018.06.008.

64. Solanas E, Sanchez-Fuentes N, Serrablo A, Lue A, Lorente S, Cortés L, et al. 2022. How donor and surgical factors affect the viability and functionality of human hepatocytes isolated From liver resections. Front Med (Lausanne) 9:875147, PMID: 35646956, https://doi.org/10.3389/fmed.2022.875147.

65. Lake AD, Novak P, Hardwick RN, Flores-Keown B, Zhao F, Klimecki WT, et al. 2014. The adaptive endoplasmic reticulum stress response to lipotoxicity in progressive human nonalcoholic fatty liver disease. Toxicol Sci 137(1):26–35, PMID: 24097666, https://doi.org/10.1093/toxsci/kft230.

66. Lee S, Kim S, Hwang S, Cherrington NJ, Ryu DY. 2017. Dysregulated expression of proteins associated with ER stress, autophagy and apoptosis in tissues from nonalcoholic fatty liver disease. Oncotarget 8(38):63370–63381, PMID: 28968997, https://doi.org/10.18632/oncotarget.18812.

67. Puri P, Mirshahi F, Cheung O, Natarajan R, Maher JW, Kellum JM, et al. 2008. Activation and dysregulation of the unfolded protein response in nonalcoholic fatty liver disease. Gastroenterology 134(2):568–576, PMID: 18082745, https://doi.org/10.1053/j.gastro.2007.10.039.

68. Arconzo M, Piccinin E, Moschetta A. 2021. Increased risk of acute liver failure by pain killer drugs in NAFLD: focus on nuclear receptors and their coactivators. Dig Liver Dis 53(1):26–34, PMID: 32546444, https://doi.org/10.1016/j.dld.2020.05.034.

69. Kučera O, Al-Dury S, Lotková H, Roušar T, Rychtrmoc D, Červinková Z. 2012. Steatotic rat hepatocytes in primary culture are more susceptible to the acute toxic effect of acetaminophen. Physiol Res 61(Suppl 2):S93–S101, PMID: 23130907, https://doi.org/10.33549/physiolres.932395.

70. Ganey PE, Luyendyk JP, Maddox JF, Roth RA. 2004. Adverse hepatic drug reactions: inflammatory episodes as consequence and contributor. Chem Biol Interact 150(1):35–51, PMID: 15522260, https://doi.org/10.1016/j.cbi.2004.09.002.

71. Wu W, Zhao L, Yang P, Zhou W, Li B, Moorhead JF, et al. 2016. Inflammatory stress sensitizes the liver to atorvastatin-induced injury in ApoE-/- mice. PLoS One 11(7):e0159512, https://doi.org/10.1371/journal.pone.0159512.

72. Li W, Cao T, Luo C, Cai J, Zhou X, Xiao X, et al. 2020. Crosstalk between ER stress, NLRP3 inflammasome, and inflammation. Appl Microbiol Biotechnol 104(14):6129–6140, PMID: 32447438, https://doi.org/10.1007/s00253-020-10614-y.